Cell Reports
Physical Science

CellPress

Electronically Controlled Regioselective Hydroarylation of *gem*-Difluoroallenes

Cheng-Qiang Wang,[1] Zhi-Qiang Li,[1] Lifang Tian,[1] Patrick J. Walsh,[2,*] and Chao Feng[1,3,*]

[1]Technical Institute of Fluorochemistry (TIF), Institute of Advanced Synthesis (IAS), School of Chemistry and Molecular Engineering, State Key Laboratory of Material-Oriented Chemical Engineering, Nanjing Tech University, 30 South Puzhu Road, Nanjing 211816, P. R. China
[2]Roy and Diana Vagelos Laboratories, Department of Chemistry, University of Pennsylvania, 231 South 34th Street, Philadelphia, PA 19104, USA
[3]Lead contact
*Correspondence: pwalsh@sas.upenn.edu (Patrick J. Walsh), iamcfeng@njtech.edu.cn (Chao Feng).

SUMMARY

All-carbon quaternary centers are ubiquitous structural motifs in natural products, bioactive molecules and pharmaceuticals. The formation of these crowded carbon centers is well known to be challenging, and methods to access them remain in high demand. Transition metal-based strategies have emerged as a powerful approach to quaternary carbons, primarily relying on cross-coupling reactions and olefin arylation processes. Herein is presented a straightforward method to create benzylic all-carbon quaternary centers employing *gem*-difluoroallenes. Features of this method include room temperature C–H functionalization, excellent regioselectivity in the insertion of *gem*-difluoroallenes, and generation of *gem*-difluoroalkene products, which have widespread applications in synthesis and pharmaceutical sciences. Mechanistic studies support a turnover limiting Rh-catalyzed C–H cleavage that likely proceeds via a concerted metallation deprotonation (CMD) pathway. Regioselective insertion of the *gem*-difluoroallene is controlled by electronic effects.

INTRODUCTION

All-carbon quaternary centers constitute a class of key structural motifs that are widespread in natural products, biologically active molecules and pharmaceuticals (Figure 1A)[1–4]. The installation of these quaternary centers represents a formidable challenge, because of severe steric constraints associated with the formation of fully substituted carbon centers[5–7]. In particular, acyclic benzylic all-carbon quaternary centers have attracted wide interest due to their applications in various industries[8,9]. Among approaches for the synthesis of benzylic quaternary centers, transition metal catalyzed cross-coupling is arguably the most effective and also holds the most promise[10,11]. Insightfully designed cross-coupling processes utilizing tertiary alkyl halides[12,13], tertiary organometallics[14-16], or tertiary carboxylic acids activated as redox-active esters[9,17] have proven remarkably successful, enabling the generation of a variety of quaternary centers bearing diverse functionality. Another strategy has been the employment of regioselective intermolecular arylation of tri- or tetrasubstituted alkenes. Recent advances in chemists' ability to control the regio- and even facial selectivity in olefin insertions have greatly increased the value of this approach[18,19]. Of note, Sigman and coworkers disclosed an elegant protocol of redox-relay oxidative coupling of aryl boronic acids with trisubstituted alkenyl alcohols. This method takes advantage of the hydroxyl substituent in order to secure reaction efficiency and selectivity (Figure 1B-1, top)[20]. This line of reactivity was further explored by Marek and coworkers in a stereodivergent construction of acyclic quaternary carbon centers using alkenylcyclopropyl carbinols as the reaction partners (bottom of Figure 1B-1)[21]. Capitalizing on the directing ability of carboxylates, the intermolecular Heck arylation of tetrasubstituted alkenes was also successfully developed by Shenvi and coworkers (Figure 1B-2)[22].

Inspired by these precedents, we envisioned developing new strategies toward all-carbon quaternary centers with two guiding principles in mind. First, to render our approach atom-economical, we were attracted to C–H activation to generate the initial transition metal–carbon bond[23]. Second, we were interested in employing readily accessible tri- or tetrasubstituted allene substrates for the subsequent metal-promoted C–C bond-formation[24–27]. We envisioned that the key to success in this endeavor would lie in devising a means to control the regioselectivity of the allene insertion[28]. Ma[29] and Glorius[30] independently demonstrated that [Rh]–Ar prefers to undergo insertion into trisubstituted allenes by placing the aryl group at the less substituted allene terminus, thus avoiding the steric penalty of formation of a quaternary center. In general, the reactivity profile in the carbometallation of allenes is dominated by steric control, leading to the generation of either linear allylation or branched alkenylation products (Figure 1B-3)[28,31–36]. We, therefore, turned to manipulating the allene's electronics to overcome the pervasive steric control. Based on our continued interest in the reactions of difluoroalkenes[37–40], we were inspired to explore the hydroarylation of *gem*-difluoroallene substrates (Figure 1B-4). Notably, in 2020 Ichikawa and coworkers[41] reported the gold-catalyzed nucleophilic addition of heteroatom nucleophiles, such as phenol, acids, amides and thiophenols, to *gem*-difluoroallene. They found the addition reaction occurred at α position when phenol and acids were employed while amide and thiophenol underwent γ-selective addition. Later our group[42] and Xu's group[43] independently disclosed the regioselective

borylcupration and silylcupration of mono- and disubstituted *gem*-difluoroallenes at the γ-position. Very recently, Shi and coworkers[44] reported an elegant ligand-controlled thiol addition of monosubstituted *gem*-difluoroallenes at the β- or γ-position. Despite these examples, the community's understanding of the unique properties of disubstituted *gem*-difluoroallenes on reactivity remains underdeveloped. Herein, we report the successful C–H functionalization/hydroarylation with readily available disubstituted *gem*-difluoroallenes. Not only does this new reaction proceed with excellent regioselectivity, enabling the formation of benzylic quaternary centers, it also produces *gem*-difluoroalkenes, which are valuable precursors for the preparation of agrochemicals, pharmaceuticals, and functional materials[45,46].

Cell Reports
Physical Science

CellPress

(A) Representative natural products and bioactive compounds with benzylic quaternary centers.

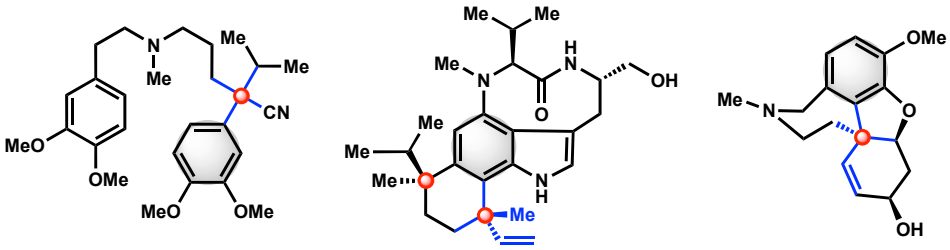

Verapamil | Teleocidin B-3 | (-)-Galantamine

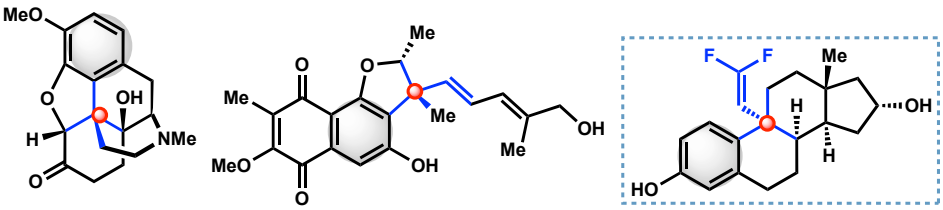

Oxycodone | Furaquinocin E | Estratriene derivative

(B) Approaches to acyclic benzylic all-carbon quaternary centers through aryl-metallation of *gem*-disubstituted C=C double bonds and reaction profiles of allene hydroarylations.

1) Redox-relay oxidative Heck arylation

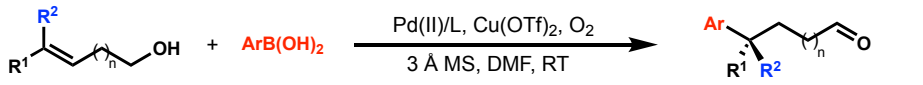

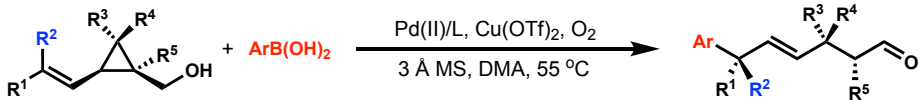

2) Directing group assisted Heck coupling

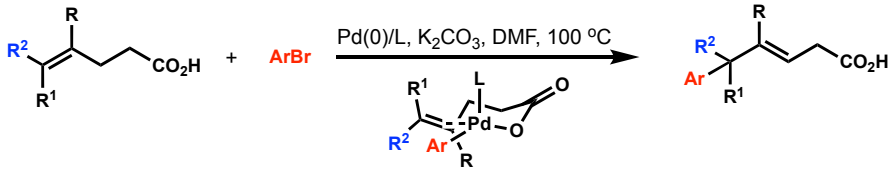

Hydroarylation of multi-substituted allenes

3) Previous work: Steric control

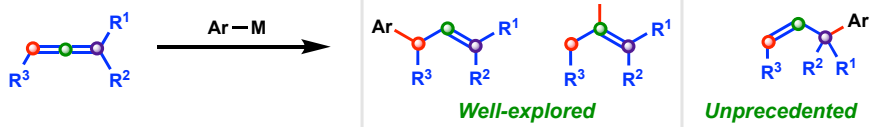

4) This work: Electronic control

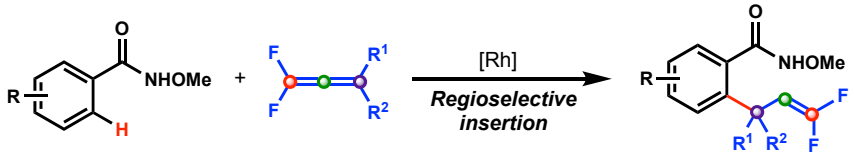

Figure 1. All-carbon quaternary benzylic centers in representative molecules and approaches to their construction

(A) Representative natural products and bioactive compounds with benzylic all-carbon quaternary centers.
(B) Approaches to acyclic benzylic all-carbon quaternary centers through aryl-metallation of *gem*-disubstituted C=C double bonds and reaction profiles of allene hydroarylations. (1) Redox-relay oxidative Heck reaction, (2) Remote directed Heck reaction, (3) Prior art in hydroarylation of allenes under steric control, (4) Capitalizing on electronic control for the regioselective construction of quaternary centers.

RESULTS AND DISCUSSION

Reaction Development and Optimization

After examination of many reaction parameters for the coupling of amide **1a** with *gem*-difluoroallene **2a**, the desired product **3aa** was ultimately isolated in 95% yield when the reaction was carried out in DCE (1,2-dichloroethane) using $[Cp^*RhCl_2]_2$ (2 mol%) and NaOAc (20 mol%) as the precatalyst and additive, respectively, at RT (28 °C) for 12 h (Table 1, entry 1) (see the Supplemental Information for details of the optimization). Interestingly, replacing the NaOAc additive with HOAc or K_2CO_3 shutdown the reaction (Table 1, entries 2–3). In contrast, use of CsOPiv (20 mol%) led to product **3aa** in 86% yield (Table 1, entry 4). For reaction solvents, substitution of mesitylene or 1,4-dioxane for DCE delivered product **3aa** in 52% and 16%, respectively (Table 1, entries 5–6). Replacing the rhodium catalyst with an iridium or ruthenium catalyst did not result in any formation of the hydroarylation product (Table 1, entries 7–8). Not surprisingly, control experiments corroborated that no reaction occurred in the absence of either $[Cp^*RhCl_2]_2$ or NaOAc (Table 1, entries 9–10).

Table 1. Reaction Conditions Optimization

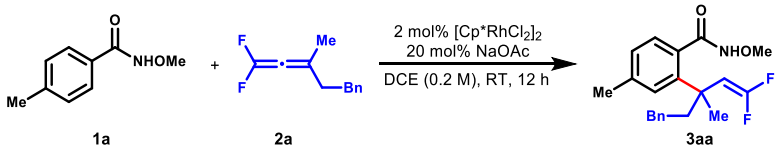

1a 2a 3aa

Entry	Deviation from standard conditions	Yield (%)
1	None	97(95)
2	HOAc vs. NaOAc	NR
3	K_2CO_3 vs. NaOAc	NR
4	CsOPiv vs. NaOAc	86
5	Mesitylene vs. DCE	52
6	1,4-Dioxane vs. DCE	16
7	$[Cp^*IrCl_2]_2$ vs. $[Cp^*RhCl_2]_2$	NR
8	$[(p\text{-cymene})RuCl_2]_2$ vs. $[Cp^*RhCl_2]_2$	NR
9	No $[Cp^*RhCl_2]_2$	NR
10	No NaOAc	NR

Reaction conditions: **1a** (0.1 mmol), **2a** (1.2 equiv), $[Cp^*RhCl_2]_2$ (2 mol%), NaOAc (20 mol%), DCE (0.5 mL), RT (28 °C), air atmosphere, 12 h. DCE, 1,2-dichloroethane, NR, no reaction. The yield was determined by crude ^1H NMR spectroscopy using 1,1,2,2-tetrachloroethane as the internal standard; isolated yield was indicated in the parenthesis.

Substrate Scope

With the optimized reaction conditions in hand (Table 1, entry 1), the reaction scope with respect to *N*-methoxy benzamide derivatives was examined using 1,1-difluoroallene **2a** (Figure 2). In general, reactions proceeded in good to excellent yields. Amides bearing substituents at the 3-position reacted with high regioselectivity at the 6-position. A variety of electron-donating substituents *meta* or *para* to the amide were well tolerated. The parent *N*-methoxy benzamide **1b** led to the formation of product **3ba** in 95% yield. Substrates bearing substituents such as 3-methyl, 4-*tert*-butyl, fused cycloalkyl and 3- or 4-methoxy groups afforded the desired products in 80–99% yields (**3ca**–**3ga**). Substrates bearing Lewis basic 4-SMe, 4-NMe_2 and 4-OAc provided products **3ha**–**3ja** in 65–79% yields. The use of biphenyl and naphthyl derived amides delivered **3ka** and **3la** in 88%

and 73% yields, respectively. Substrates containing alkene or alkyne moieties did not interfere with the hydroarylation, and the corresponding products (**3ma** and **3na**) were isolated in 76–78% yields. When *N*-methoxy benzamides with strongly electron-withdrawing substituents (4-Ac, 4-CO_2Me, 4-NO_2, 4-CN, 4-CF_3) were subjected to the standard reaction conditions, the products were obtained in 42–71% yields. In some cases, the yields with strongly electron-withdrawing groups are lower due to formation of the regioisomeric insertion products. For example, with an -NO_2 group, **3qa** and **3qa'** formed with a regioisomeric ratio of 1.5 : 1. Interestingly, a 4-CN group caused the regioisomeric ratio to invert, favoring the opposite insertion product (**3ra** : **3ra'** = 1 : 1.2, see the Supplemental Information for further details).

Substrates bearing halogens, such as 4-Cl, 4-Br, 3-Br, and 3-I underwent the hydroarylation reaction in 61–77% yields. These substrates are primed for further functionalization at the C–X bond through cross-coupling reactions. Substrates supporting benzylic functional groups often exhibit increased reactivity. In our system, benzylic functional groups such as –OH, –OC(O)H, –Cl, and –N_3 were all tolerated, affording products (**3xa**–**3aaa**) in 66–81% yields. Coupling partners containing 4-$SiMe_3$ and 4-Bpin also performed well (**3aba**; 91%, **3aca**; 75%), providing opportunities for further elaboration through well-developed metal catalyzed processes.

An amide supporting an NHBoc proved to be an excellent substrate, exhibiting high chemoselectivity in the generation of **3ada** (97% yield) with no interference from the NHBoc group. A structurally complex estrone-derivative amide **1ae** was tested. This substrate also hosts two inequivalent C–H bonds *ortho* to the amide. Nonetheless, functionalization occurred regioselectively at the least hindered position to provide the *gem*-difluoroalkene **3aea** in 80% yield. In addition, amides derived from Pterostilbene and Cholesteryl chloroformate with alkene and carbonate moieties were also investigated, delivering the expected hydroarylation products **3afa** and **3aga** in 73–75% yields. The successful generation of these natural product derivatives underscores the potential applicability of this method to late-stage elaboration of complex molecules.

Heterocycles are the bread and butter of the pharmaceutical industry, with pyridyl groups being among the most common[47,48]. We, therefore, examined a series of heterocycle-containing amides, beginning with **1ah** bearing a pyridyl group situated *meta* with respect to the *N*-methoxy amide. Compound **1ah** contains two different C–H bonds *ortho* to the directing group. This substrate underwent regioselective C–H activation at the more acidic site, providing the product **3aha** in 76% yield with excellent regioselectivity. This substrate also contains a sensitive 2-chloropyridyl group that can be easily elaborated. In pyridine derivative **1ai**, selectivity in the C–H activation is observed at the sterically more accessible site. The quaternary center-containing product was isolated in 62% yield, while the minor isomer formed in 23% (rr~2.7:1, regioisomeric ratio). The *N*-methoxyquinoline-7-carboxamide reacted to afford the desired product **3aja** in 51% yield. Thiophene derivatives were also viable, generating the heterocyclic products **3aka** and **3ala** in 73–76% yields. Natural product-derived **1am**, containing a tetrahydropyran, furnished **3ama** in 83% yield. Complex substrates originating from a coumarin derivative and Amoxapine were also well accommodated and afforded the desired products **3ana**–**3aoa** in 62–71% yields. These results indicate that a variety of heterocycles are compatible with this method.

We next set out to examine the reaction generality with regard to the 1,1-difluoroallenes using amide **1a**. As depicted in Figure 3, an array of the 1,1-difluoroallene derivatives successfully engaged in this transformation and delivered the designed products in moderate to high yields. Allene substrates bearing a variety of electron-rich or electron-poor aryl rings, such as ether, siloxane, CF_3, Br, and alkynyl groups, participated in the hydroarylation reaction and delivered the corresponding *gem*-difluoroalkene products **3ab**–**3ah** in 78–95% yields. The electron rich thiophene-derivative **2i** reacted smoothly to afford product **3ai** in 85% yield. 1,1-Diflouroallene **2j**, bearing a bromo indole, was more challenging but afforded desired product **3aj** in a workable 45% yield. An allene bearing a 4-methoxy benzyl group (**2k**) also underwent reaction giving **3ak** (62% yield). *gem*-Difluoroallenes with alicyclic structures were amenable to this reaction giving **3al** and **3am** in 74% and 49% yield, respectively. The structure of **3al** was confirmed by X-ray crystallographic analysis (CCDC 1911766). *gem*-Difluoroallenes containing two aliphatic groups (**2n**) and those with remote alkenyl, ether, chloro and silyl-ether substituents all proved to be viable substrates, with the products being obtained in 42–96% yields (**3ao**–**3aw**).

Cell Reports
Physical Science

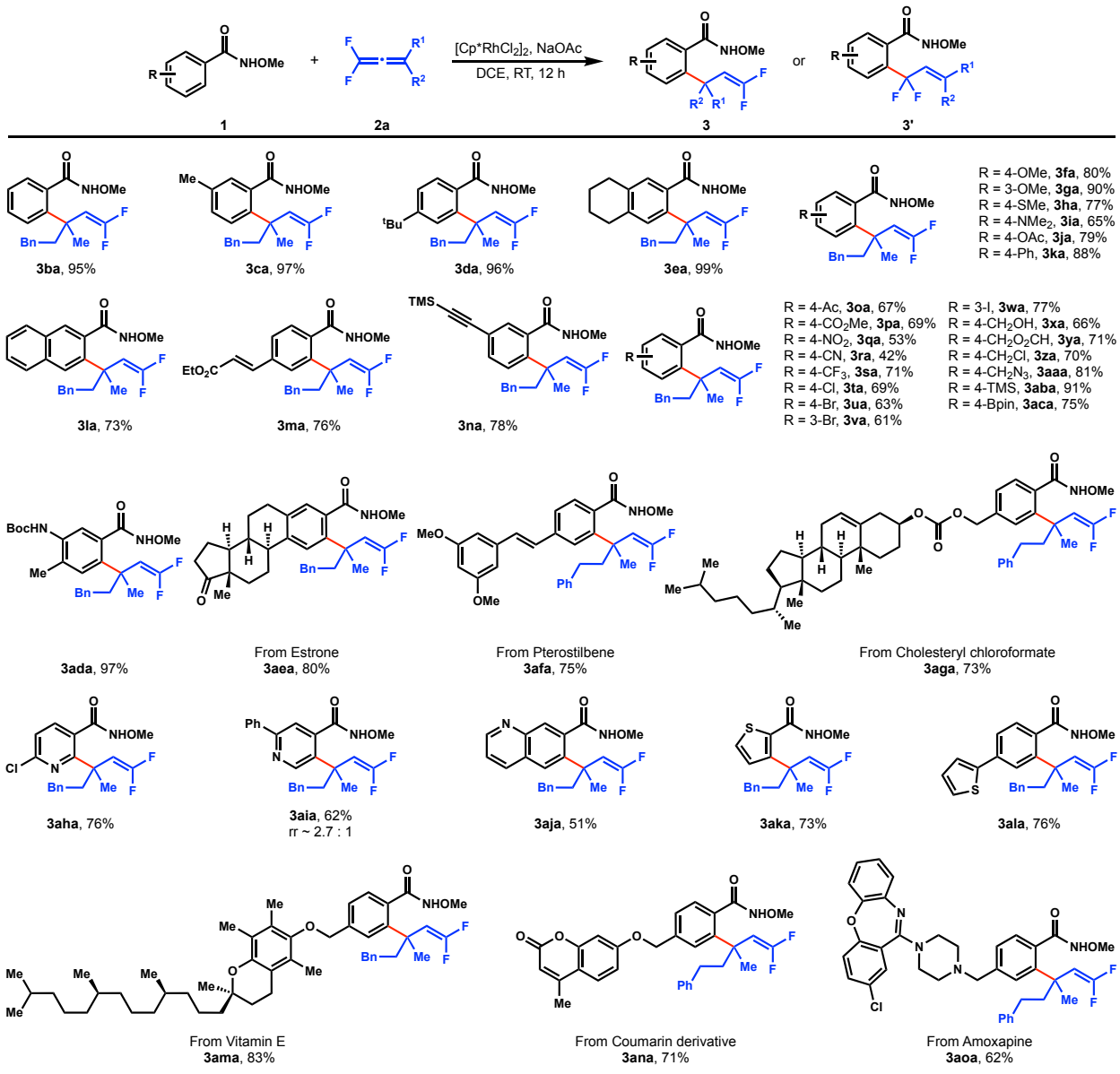

Figure 2. Scope of *N*-methoxy benzamide derivatives

Benzylic all-carbon quaternary center construction via hydroarylation of 1,1-difluoroallene **2a** using different *N*-methoxy benzamide derivatives. Reaction conditions: **1** (0.1 mmol), **2a** (1.2 equiv), $[Cp^*RhCl_2]_2$ (2 mol%), NaOAc (20 mol%), DCE (0.5 mL), RT (28 °C), air atmosphere, 12 h, isolated yields. See the Supplemental Information for reaction details.

Cell Reports
Physical Science

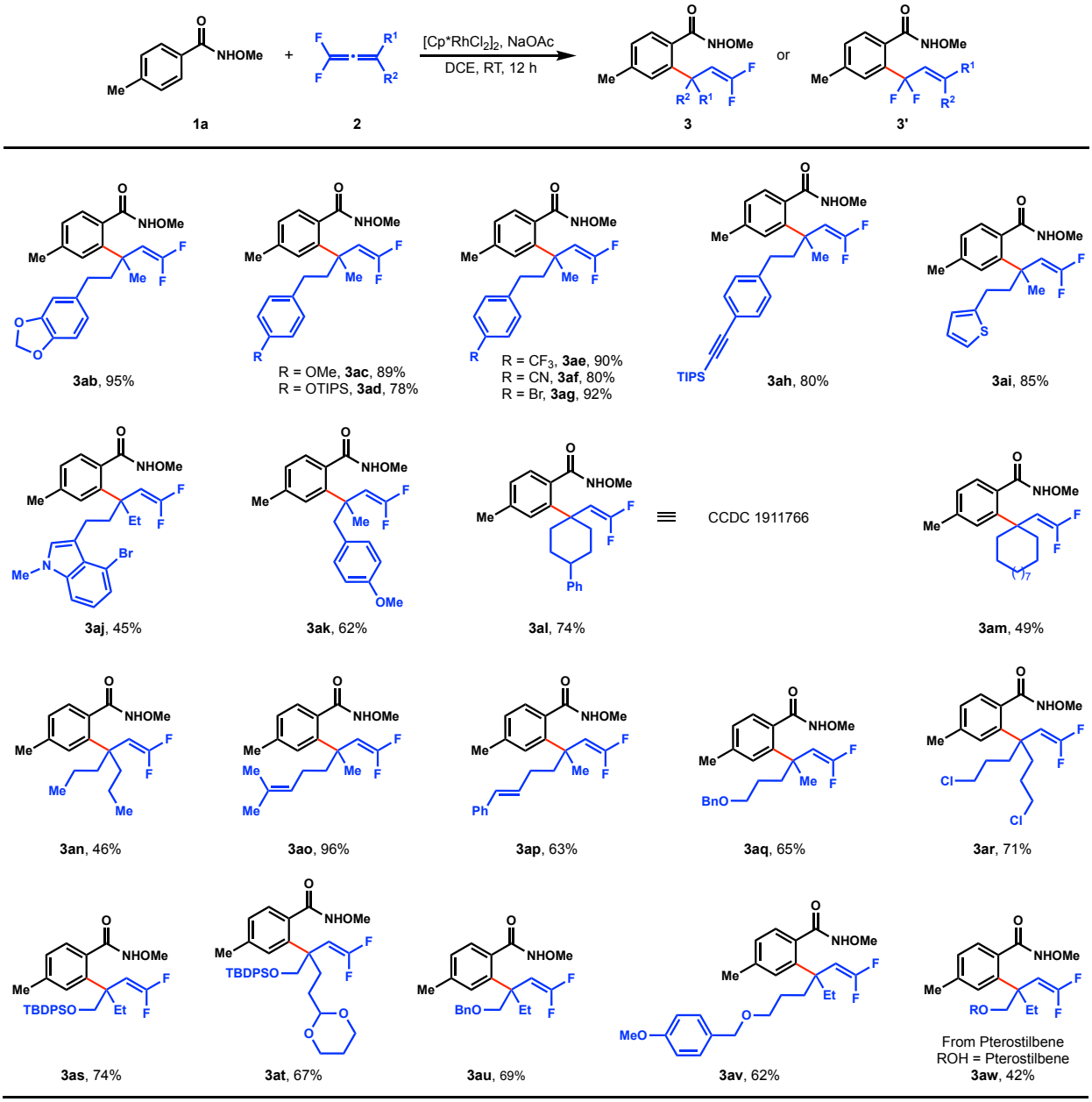

Figure 3. Scope of 1,1-difluoroallenes

Benzylic all-carbon quaternary center construction via hydroarylation of various 1,1-difluoroallenes **2** with amide **1a**. Reaction conditions: **1a** (0.1 mmol), **2** (1.2 equiv), $[Cp^*RhCl_2]_2$ (2 mol%), NaOAc (20 mol%), DCE (0.5 mL), RT (28 °C), air atmosphere, 12 h, isolated yields. CCDC, Cambridge Crystallographic Data Centre. See the Supplemental Information for reaction details.

Gram Scale Reaction

To further showcase the practicality of this transformation, a gram-scale reaction between amide **1a** and 1,1-difluoroallene **2a** was carried out, which delivered the desired product **3aa** in 88% yield (Figure 4). This yield compares favorably to the 0.1 mmol scale reaction (95% yield) (for full details see the Supplemental Information).

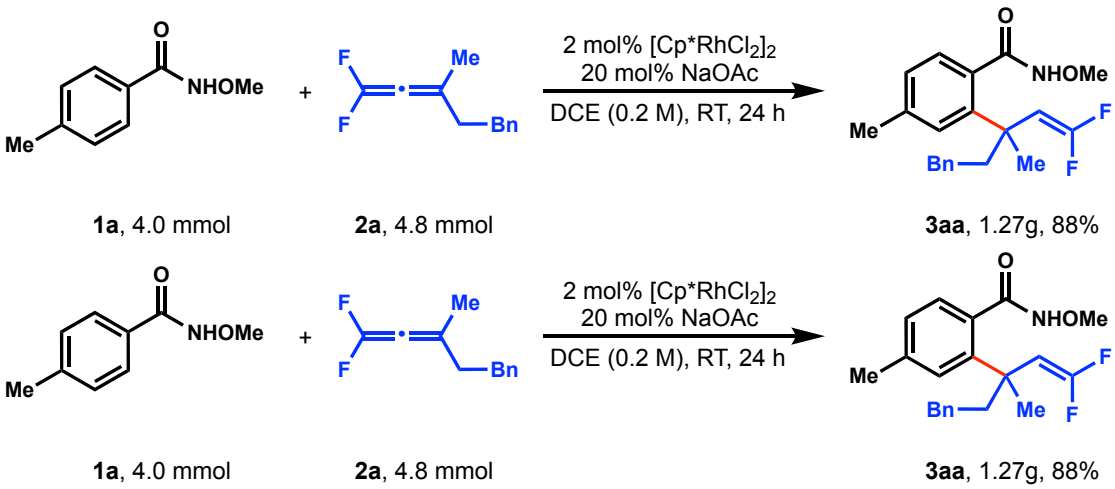

Figure 4. Gram-scale reaction

Gram-scale reaction between amide **1a** and 1,1-difluoroallene **2a**.

Synthetic Transformations

To showcase the potential utility of the *gem*-difluoroalkene products **3**, several transformations were conducted (Figure 5) focusing on taking advantage of the utility of the directing group. The halonium-induced annulation of **3aa** using *N*-iodosuccinimide provided the seven-membered heterocyclic product **6** in 65% yield (dr = 3.3 : 1, dr: diastereomeric ratio), which bears a *gem*-difluoromethylene unit (Figure 5a). Treatment of **3aa** with TBAF in MeOH at 80 °C afforded the mono-fluoroalkenyl-containing macrolactam **7** in 76% yield (Figure 5b), whereas spirocyclic *N*-methoxybenzimidate derivative **8** was obtained in 86% yield when **3aj** was treated with AgF and 3 Å molecular sieves in DMSO at 80 °C (Figure 5c). The structure of **8** was confirmed by X-ray crystallographic analysis (CCDC 1911772). In addition, triazole **10** could be generated in good yield from **3ag** through a one-pot cascade reaction comprising desilylation, intramolecular annulation/copper-catalyzed azide-alkyne cycloaddition (Figure 5d, for full details see the Supplemental Information). The reduction of Weinreb amide derived from **3aa** using $LiAlH_4$ as the reductant afforded benzylic amine **12** bearing a mono-fluoroalkene unit in good yield (Figure 5e). The hydrolysis of **3aa** formed indanone **13** in 65% yield (Figure 5f), which could be further oxidized to the corresponding six-membered lactone **14** (Figure 5g). Of note, the above transformations all incorporate the directing group in a productive fashion, via intramolecular or intermolecular reactions. The resulting compounds are potentially bioactive, containing a benzylic all-carbon quaternary center that are usually difficult to access.

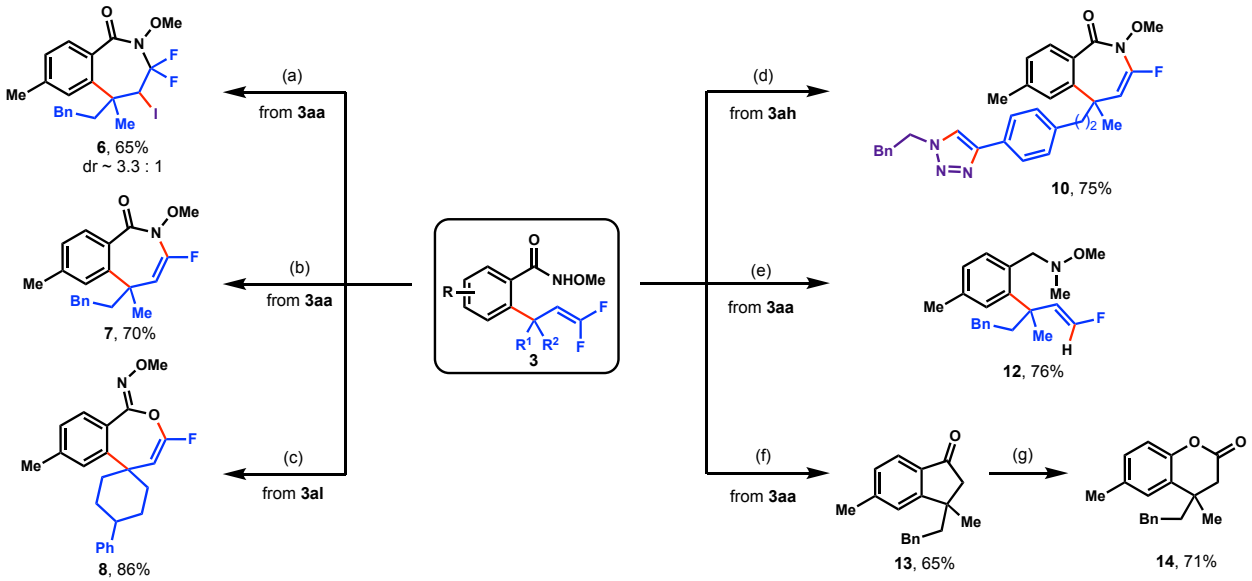

Figure 5. Synthetic transformations

Synthetic transformations of the obtained *gem*-difluoroalkene products **3**.
(A) NIS, MeCN/H_2O, 40 °C.
(B) TBAF, MeOH, 80 °C.
(C) AgF, DMSO, 3Å MS, 80 °C.
(D) (1) TBAF, THF, RT; (2) $CuSO_4$, Sodium Ascorbate, $BnCH_2N_3$, THF/H_2O, RT.
(E) (1) NaH, MeI, THF, 0 °C to RT; (2) $LiAlH_4$, THF, 80 °C.
(F) HCl (6 M), HOAc, 125 °C.
(G) TsOH, m-CPBA, DCM, 0 °C to RT.

Mechanistic Studies

To probe the reaction mechanism, a series of experiments were conducted (Figure 6). An intermolecular kinetic isotope effect experiment with 1 equiv each of **1b** and **1b-*d*$_5$** afforded a KIE value of 13 (Figure 6a) and the parallel experimental KIE has a value of 2.5 (Figure 6b), which indicates that C–H bond cleavage is involved in the turnover-limiting step. We next wanted to explore the source of the proton in the formation of the sp^2 C–H bond. Thus, addition of D_2O (5 equiv relative to **1a**) to the reaction of **1a** and **2a** under otherwise standard conditions gave the product **3aa-*d*$_1$** with 24% deuterium incorporation at the olefinic position (the proton can come from the N–H and the *ortho*-C–H that was activated). This observation suggests that protodemetalation is involved in liberating the product from the rhodium center (Figure 6c).

To determine whether the *gem*-difluorosubstituents are responsible for the formation of benzylic quaternary centers, several experiments were performed. In accordance with Ma's pioneering studies, the non-fluorinated allene **2x** was also viable under our conditions and led to the generation of hydroarylation product **4ax** (45% yield, Figure 6d)[29]. The absence of the quaternary center-containing product is consistent with the regioselectivity observed by Ma and co-workers and highlights the important role of the fluoride substituents in defining the regioselectivity of our reaction. Surprisingly, substitution of 1,1-dibromoallene **2y** for 1,1-difluoroallene **2a**, resulted in no reaction. This result likewise emphasizes the importance of the *gem*-difluorosubstituents in this reaction (Figure 6e)[42,49–52]. To further probe the influence of *gem*-dialkyl substituents on the migratory insertion, we conducted the reaction with the monoalkyl difluoroallene **2z**. Interestingly this substrate did not react under the standard conditions (Figure 6f). It is possible that a single alkyl is not sufficient to stabilize a partial positive charge in the transition state (see below, Figure 7).

Cell Reports
Physical Science

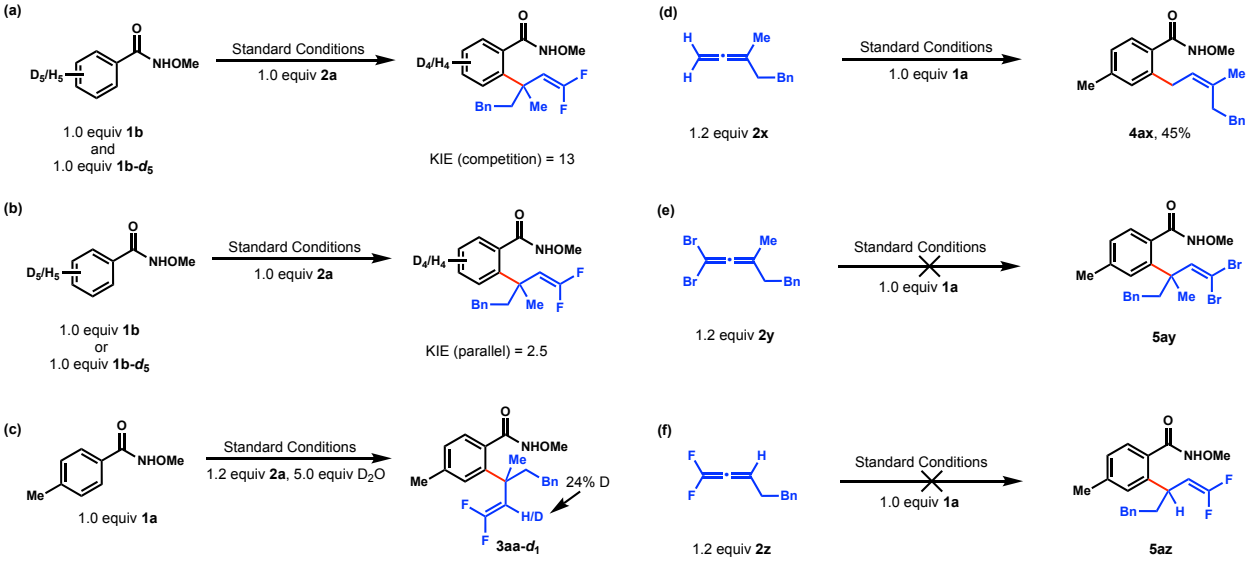

Figure 6. Mechanistic studies

Mechanistic studies of the rhodium-catalyzed hydroarylation of allenes.
(A) Intermolecular kinetic isotope effect experiment among amide **1b**, **1b-*d*$_5$** and allene **2a**.
(B) Parallel KIE experiments (reaction between amide **1b** and allene **2a**, reaction between amide **1b-*d*$_5$** and allene **2a**).
(C) Deuterium incorporation experiment.
(D) Reaction between amide **1a** and terminal allene **2x**.
(E) Reaction between amide **1a** and gem-dibromoallene **2y**.
(F) Reaction between amide **1a** and monoalkyl difluoroallene **2z**.

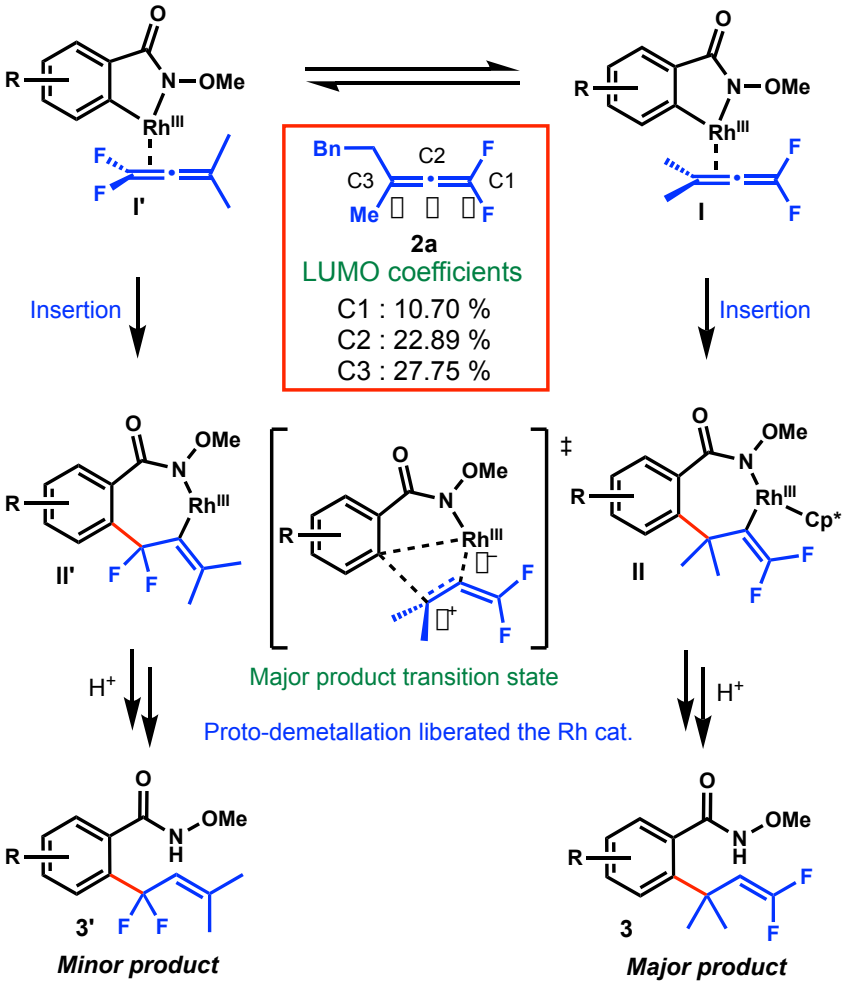

Figure 7. Key steps in the proposed reaction mechanism

The LUMO coefficients of allene **2a** and key steps in a plausible mechanism.

To explain the unusual regioselectivity of *gem*-difluoroallenes we have conducted DFT calculations to understand the frontier molecular orbitals of substrate **2a**. The DFT calculations were performed with the Gaussian 09 program[53]. Geometries of the minimum energy structures were optimized at the B3-LYP level of theory with the 6-31G(d, p) basis set in DCE implicitly[54–56]. As demonstrated in Figure 7, the highest contribution of LUMO orbital is located at γ position of the allene (C3 site), which is also the reaction site of this arylation. Therefore, we deduced that regioselectivity of the arylation was under an orbital control scenario[27].

On the basis of the experimental results outlined above, a plausible reaction pathway is proposed. The Rh(III)-catalyzed C–H bond activation to generate the rhodacyclic intermediate (Figure 7) is well-documented[57–61]. The coordination of *gem*-difluoroallene **2** to the Rh(III) center can be envisioned to occur at either allene π-bond, leading to intermediates **I** and **I'**. The *gem*-difluoro substituents cause the neighboring π-bond to be a poor donor and stronger π-acceptor. We hypothesize that the Rh(III)-based metallocycle **I** is electron deficient and, as such, preferentially coordinates to the more electron-rich dialkyl-substituted π-bond. In most cases, insertion occurs readily to generate the quaternary center, which is followed by two proto-demetallations of the type observed in Figure 6c with liberation of the catalyst.

In the case of amide substrates with strongly electron withdrawing groups, such as NO_2 and CN (**3qa** and **3ra**), the observation of differing amount of difluoroalkylation products **3'** could be interpreted by assuming the lower migratory aptitude of aryl-migration of electron-deficient aryl motif compared with that of electron-rich ones. On the other hand, the more polarized C-

Rh bond caused by strongly electron withdrawing groups might entail a scenario of charge-controlled insertion, thus bring forth such a situation that migratory insertion through either **II** or **II'** would coexist and compete with each other. Taken together, the predominant production of compound **3** is attributed to the intrinsic electronic effect endowed by the *gem*-difluorosubstituents, which overrides otherwise prevailing steric control observed in cases of allene hydroarylation reactions.

In summary, a straightforward and fully atom-economical protocol for the efficient assembly of benzylic quaternary centers has been successfully developed. Employing the commercially available Rh(III) catalyst precursor $[Cp^*RhCl_2]_2$ and NaOAc, a catalytic C–H functionalization/hydroarylation of 3,3-dialkyl-substituted 1,1-difluoroallenes with *N*-methoxy benzamides under mild reaction conditions was introduced that is tolerant of a wide array of functional groups. Not only is this approach toward benzylic quaternary centers unique, the products also contain *gem*-difluoroalkenes, which are valued building blocks in the pharmaceutical and material sciences. The success of this method is attributed to the unique effect of fluoro substituents on allene substrates, that is responsible for guiding the distinct regioselectivity in the carbometallation step. The highly regioselective hydrometallation observed with the *gem*-difluoroallenes herein stands in sharp contrast to the reports on the hydroarylation of non-fluorinated allene substrates. Given the importance of fluorinated compounds, the generality of this method, and the new chemical space accessible with this hydroarylation, we anticipate that this chemistry will be attractive to practitioners in the field of drug discovery.

EXPERIMENTAL PROCEDURES

Resource Availability

Lead Contact

Further information and requests for resources should be directed to and will be fulfilled by the lead contact, Chao Feng (iamcfeng@njtech.edu.cn).

Materials Availability

All other data supporting the findings of this study are available within the article and the supplemental information or from the lead contact upon reasonable request.

Data and Code Availability

The authors declare that the data supporting the findings of this study are available within the article and its supplemental information files as well as from the corresponding author on request. Crystallographic data are available from the Cambridge Crystallographic Data Centre with the following codes: **3aj** (CCDC 1911766), **8** (CCDC 1911772) and **9** (CCDC 1911773, see the Supplemental Information for the detailed chemical structure of **9**).

SUPPLEMENTAL INFORMATION

Supplemental Information contains Supplemental Experimental Procedures, Supplemental Figures S1-S234 and Supplemental Tables S1-S6, which can be found online at

ACKNOWLEDGMENTS

We gratefully acknowledge the financial support of the National Natural Science Foundation of China (21871138) and the Distinguished Youth Foundation of Jiangsu Province. P.J.W. thanks the US National Science Foundation for generous support (CHE- 2154593). We are grateful to Prof. Xiao-Ming Ren (Nanjing Tech University) and Prof. Yang Zou (Nanjing Tech University) for the X-ray crystallographic analyses.

AUTHOR CONTRIBUTIONS

C.-Q.W. performed most of the experiments and mechanistic study. Z.-Q.L. took part in the preparation of some substrates. L.T. did the density functional theory calculations. P.J.W. discussed the chemistry, suggested experiments and revised the manuscript. C.F. conceived the study, directed the project and wrote the manuscript with the assistance of C.-Q.W.

DECLARATION OF INTERESTS

C.F. and C.-Q.W. are inventors on a Chinese patent related to this work (CN 110003042 A, 12 July 2019). The other authors declare that they have no competing interests.

REFERENCES

1. Ling, T., and Rivas, F. (2016). All-carbon quaternary centers in natural products and medicinal chemistry: Recent advances. Tetrahedron *72*, 6729–6777.

2. Zi, W., Zuo, Z., and Ma, D. (2015). Intramolecular dearomative oxidative coupling of indoles: A unified strategy for the total synthesis of indoline alkaloids. Acc. Chem. Res. *48*, 702–711.

3. Quasdorf, K. W., and Overman, L. E. (2014). Catalytic enantioselective synthesis of quaternary carbon stereocentres. Nature *516*, 181–191.

4. Long, R., Huang, J., Gong, J., and Yang, Z. (2015). Direct construction of vicinal all-carbon quaternary stereocenters in natural product synthesis. Nat. Prod. Rep. *32*, 1584–1601.

5. Bhat, V., Welin, E. R., Guo, X., and Stoltz, B. M. (2017). Advances in stereoconvergent catalysis from 2005 to 2015: Transition-metal-mediated stereoablative reactions, dynamic kinetic resolutions, and dynamic kinetic asymmetric transformations. Chem. Rev. *117*, 4528–4561.

6. Vasseur, A., and Marek, I. (2017). Merging allylic C–H bond activation and C–C bond cleavage en route to the formation of a quaternary carbon stereocenter in acyclic systems. Nat. Protoc. *12*, 74–87.

7. Feng, J., Holmes, M., and Krische, M. J. (2017). Acyclic quaternary carbon stereocenters via enantioselective transition metal catalysis. Chem. Rev. *117*, 12564–12580.

8. Marson, C. M. (2017). New and unusual scaffolds in medicinal chemistry. Chem. Soc. Rev. *40*, 5514–5533.

9. Chen, T.-G., Zhang, H., Mykhailiuk, P. K., Merchant, R. R., Smith, C. A., Qin, T., and Baran P. S. (2019). Quaternary centers by nickel-catalyzed cross-coupling of tertiary carboxylic acids and (hetero)aryl zinc reagents. Angew. Chem., Int. Ed. *58*, 2454–2458.

10. Liu, Y., Han, S.-J., Liu, W.-B., and Stoltz, B. M. (2015). Catalytic enantioselective construction of quaternary stereocenters: Assembly of key building blocks for the synthesis of biologically active molecules. Acc. Chem. Res. *48*, 740–751.

11. Marek, I., Minko, Y., Pasco, M., Mejuch, T., Gilboa, N., Chechik, H., and Das, J. P. (2014). All-carbon quaternary stereogenic centers in acyclic systems through the creation of several C–C bonds per chemical step. J. Am. Chem. Soc. *136*, 2682–2694.

12. Zultanski, S. L., and Fu, G. C. (2013). Nickel-catalyzed carbon–carbon bond-forming reactions of unactivated tertiary alkyl halides: Suzuki arylations. J. Am. Chem. Soc. *135*, 624–627.

13. Wang, X., Ma, G., Peng, Y., Pitsch, C. E., Moll, B. J., Ly, T. D., Wang, X., and Gong, H. (2018). Ni-catalyzed reductive coupling of electron-rich aryl iodides with tertiary alkyl halides. J. Am. Chem. Soc. *140*, 14490–14497.

14. Cheng, F.; Lu, W.; Huang, W.; Wen, L.; Li, M., and Meng, F. (2018). Cu-catalyzed enantioselective synthesis of tertiary benzylic copper complexes and their in situ addition to carbonyl compounds. Chem. Sci. *9*, 4992-4998.

15. Primer, D. N., and Molander, G. A. (2017). Enabling the cross-coupling of tertiary organoboron nucleophiles through radical-mediated alkyl transfer. J. Am. Chem. Soc. *139*, 9847–9850.

16. Zhang, S., Kim, B.-S., Wu, C., Mao, J., and Walsh, P. J. (2017). Palladium-catalysed synthesis of triaryl(heteroaryl)methanes. Nat. Commun. *8*, 14641.

17. Toriyama, F., Cornella, J., Wimmer, L., Chen, T.-G., Dixon, D. D., Creech, G., and Baran, P. S. (2016). Redox-active esters in Fe-catalyzed C–C coupling. J. Am. Chem. Soc. *138*, 11132–11135.

18. Shibasaki, M., Vogl, E. M., and Ohshima, T. (2004). Asymmetric Heck reaction. Adv. Synth. Catal. *346*, 1533–1552.

19. Namyslo, J. C., Storsberg, J., Klinge, J., Gärtner, C., Yao, M.-L., Ocal, N., and Kaufmann, D. E. (2010). The hydroarylation reaction—scope and limitations. Molecules *15*, 3402–3410.

20. Mei, T.-S., Patel, H. H., and Sigman, M. S. (2014). Enantioselective construction of remote quaternary stereocentres. Nature *508*, 340–344.

21. Bruffaerts, J., Pierrot, D., and Marek, I. (2018). Efficient and stereodivergent synthesis of unsaturated acyclic fragments bearing contiguous stereogenic elements. Nat. Chem. *10*, 1164–1170.

22. Huffman, T. R., Wu, Y., Emmerich, A., and Shenvi, R. A. (2019). Intermolecular Heck coupling with hindered alkenes directed by potassium carboxylates. Angew. Chem., Int. Ed. *58*, 2371–2376.

23. Li, Y., and Xu, S. (2018). Transition-metal-catalyzed C–H functionalization for construction of quaternary carbon centers. Chem. Eur. J. *24*, 16218–16245.

24. Zhu, C., Schwarz, J. L., Cembellín, S., Greßies, S., and Glorius, F. (2018). Highly selective manganese(I)/Lewis acid cocatalyzed direct C–H propargylation using bromoallenes. Angew. Chem., Int. Ed. *57*, 437–441.

25. Holmes, M., Schwartz, L. A., and Krische, M. J. (2018). Intermolecular metal-catalyzed reductive coupling of dienes, allenes, and enynes with carbonyl compounds and imines. Chem. Rev. *118*, 6026–6052.

26. Mae, M., Hong, J. A., Xu, B., and Hammond, G. B. (2006). Highly regioselective synthesis of *gem*-difluoroallenes through magnesium organocuprate SN2' substitution. Org. Lett. *8*, 479–482.

27. Fuchibe, K., Ueda, M., Yokota, M., and Ichikawa, J. (2012). γ-Selective addition to 1,1-difluoroallenes: Three-component coupling leading to 2,2-disubstituted 1,1-difluoroalkenes. Chem. Lett. *41*, 1619–1621.

28. Santhoshkumar, R., and Cheng, C.-H. (2018). Fickle reactivity of allenes in transition-metal-catalyzed C–H functionalizations. Asian J. Org. Chem. *7*, 1151–1163.

29. Zeng, R., Fu, C., and Ma, S. (2012). Highly selective mild stepwise allylation of N-methoxybenzamides with allenes. J. Am. Chem. Soc. *134*, 9597–9600.

30. Wang, H., and Glorius, F. (2012). Mild rhodium(III)-catalyzed C–H activation and intermolecular annulation with allenes. Angew. Chem., Int. Ed. *51*, 7318–7322.

31. Nakanowatari, S., Mei, R., Feldt, M., and Ackermann, L. (2017). Cobalt(III)-catalyzed hydroarylation of allenes via C–H activation. ACS. Catal. *7*, 2511–2515.

32. Wang, C., Wang, A., and Rueping, M. (2017). Manganese-catalyzed C–H functionalizations: Hydroarylations and alkenylations involving an unexpected heteroaryl shift. Angew. Chem., Int. Ed. *56*, 9935–9538.

33. Zeldin, R. M., and Toste, F. D. (2011). Synthesis of flinderoles B and C by a gold-catalyzed allene hydroarylation. Chem. Sci. *2*, 1706–1709.

34. Zeng, R., Ye, J., Fu, C., and Ma, S. (2013). Arene C–H bond functionalization coupling with cyclization of allenes. Adv. Synth. Catal. *355*, 1963–1970.

35. Gong, T.-J., Su, W., Liu, Z.-J., Cheng, W.-M., Xiao, B., and Fu, Y. (2014). Rh(III)-catalyzed C–H activation with allenes to synthesize conjugated olefins. Org. Lett. *16*, 330–333.

36. Ye, B., and Cramer, N. (2013). A tunable class of chiral Cp ligands for enantioselective rhodium(III)-catalyzed C–H allylations of benzamides. J. Am. Chem. Soc. *135*, 636–639.

37. Tian, P., Feng, C., and Loh, T.-P. (2015). Rhodium-catalysed C(sp2)–C(sp2) bond formation via C–H/C–F activation. Nat. Commun. *6*, 7472.

38. Tian, P., Wang, C.-Q., Cai, S.-H., Song, S., Ye, L., Feng, C., and Loh, T.-P. (2016). F^- nucleophilic-addition-induced allylic alkylation. J. Am. Chem. Soc. *138*, 15869–15872.

39. Zhu, C., Song, S., Zhou, L., Wang, D.-X., Feng, C., and Loh, T.-P. (2017). Nonconventional difluoroalkylation of C(sp2)–H bonds through hydroarylation. Chem. Commun. *53*, 9482–9485.

40. Zhu, C., Liu, Z.-Y., Tang, L., Zhang, H., Zhang, Y.-F., Walsh, P. J., and Feng, C. (2020). Migratory functionalization of unactivated alkyl bromides for construction of all-carbon quaternary centers via transposed *tert*-C-radicals. Nat. Commun. *11*, 4860.

41. Fuchibe, K., Abe, M., Sasaki, M., and Ichikawa, J. (2020). Gold-catalyzed electrophilic activation of 1,1-difluoroallenes: *α*- and *γ*-selective addition of heteroatom nucleophiles. J. Fluor. Chem. *232*, 109452.

42. Wang, C.-Q., Li, Y., and Feng, C. (2021). Sterically congested boronate and silane synthesis via electronically controlled protoboration and protosilylation. Cell Rep. Phys. Sci. *2*, 10641.

43. Shan, C.-C., Dai, K.-Y., Zhao, M., and Xu, Y.-H. (2021). Copper catalyzed protosilylation/protoborylation of *gem*-difluoroallenes. Eur. J. Org. Chem. 4054–4058.

44. Han, X., Wang, M., Liang, Y., Zhao, Y., and Shi, Z. (2022). Regio- and enantioselective nucleophilic addition to *gem*-difluoroallenes. Nat. Synth. *1*, 227–234.

45. Chelucci, G. (2012). Synthesis and metal-catalyzed reactions of *gem*-dihalovinyl systems. Chem. Rev. *112*, 1344–1462.

46. Zhang, X., and Cao, S. (2017). Recent advances in the synthesis and C–F functionalization of *gem*-difluoroalkenes. Tetrahedron Lett. *58*, 375–392.

47. Vitaku, E., Smith, D. T., and Njardarson, J. T. (2014). Analysis of the structural diversity, substitution patterns, and frequency of nitrogen heterocycles among U.S. FDA approved pharmaceuticals. J. Med. Chem. *57*, 10257–10274.

48. Taylor, R. D., MacCoss, M., and Lawson, A. D. G. (2014). Rings in drugs. J. Med. Chem. *57*, 5845–5859.

49. Wang, C.-Q., Ye, L., Feng, C., and Loh T.-P. (2017). C–F bond cleavage enabled redox-neutral [4+1] annulation via C–H bond activation. J. Am. Chem. Soc. *139*, 1762–1765.

50. Orsi, D. L., and Altman, R. A. (2017). Exploiting the unusual effects of fluorine in methodology. Chem. Commun. *53*, 7168–7181. 51. Wang, C.-Q., Zhang, Y., and Feng, C. (2017). Fluorine effects on group migration via a rhodium(V) nitrenoid intermediate. Angew. Chem., Int. Ed. *56*, 14918–14922.

52. Ni, C., and Hu, J. (2016). The unique fluorine effects in organic reactions: Recent facts and insights into fluoroalkylations. Chem. Soc. Rev. *45*, 5441–5454.

53. Frischi, M. J., Trucks, G. W., Schlegel, H. B., Scuseria, G. E., Robb, M. A., Cheeseman, J. R., Scalmani, G., Barone, V., Mennucii, B., Petersson, G. A., et al. Gaussian 09, Revision D.01.

54. Ditcrfield, R., Herre, W. J., and Pople, J. A. (1971). Self-consistent molecular-orbital methods. IX. An extended Gaussian-type basis for molecular-orbital studies of organic molecules. J. Chem. Phys. *54*, 724–728.

55. Herre, W. J., itcrfield, R., and Pople, J. A. (1972). Self-consistent molecular orbital methods. XII. Further extensions of Gaussian-type basis sets for use in molecular orbital studies of organic molecules. J. Chem. Phys. *56*, 2257–2261.

56. Becke A. D. (1993). Densit.y-functional thermochemistry. III. The role of exact exchange. J. Chem. Phys. *98*, 5648–5652.

57. Colby, D. A., Bergman, R. G., and Ellman, J. A. (2010). Rhodium-catalyzed C–C bond formation via heteroatom-directed C–H bond activation. Chem. Rev. *110*, 624–655.

58. Song, G., Wang, F., and Li, X. (2012). C–C, C–O and C–N bond formation via rhodium(III)-catalyzed oxidative C–H activation. Chem. Soc. Rev. *41*, 3651–3678.

59. Ye, B., and Cramer, N. (2015). Chiral cyclopentadienyls: Enabling ligands for asymmetric Rh(III)-catalyzed C–H functionalizations. Acc. Chem. Res. *48*, 1308–1318.

60. Vásquez-Céspedes, S., Wang, X., and Glorius, F. (2018). Plausible Rh(V) intermediates in catalytic C–H activation reactions. ACS Catal. *8*, 242–257.

61. Piou, T., and Rovis, T. (2018). Electronic and steric tuning of a prototypical piano stool complex: Rh(III) catalysis for C–H functionalization. Acc. Chem. Res. *51*, 170–180.